(Received 7 September 2024, Accepted 29 October 2024, Scheduled 10 November 2024)

Flexible Ring Slot Antenna for Optimized 5G Performance in N77 and N78 Frequency Bands for Wearable Applications

Gaurav Kumar Soni[1], Dinesh Yadav[1,*], Ashok Kumar[2], Chanchal Sharma[3], and Manish Varun Yadav[4]

[1]*Department of Electronics and Communication Engineering, Manipal University Jaipur, Jaipur, Rajasthan, India*
[2]*Department of Electronics and Communication Engineering, Government Mahila Engineering College, Ajmer, Rajasthan, India*
[3]*Department of Computer Science Engineering in Artificial Intelligence and Machine Learning, Saraswati College of Engineering, Navi Mumbai, Maharashtra, India*
[4]*Department of Aeronautical and Automobile Engineering, Manipal Institute of Technology Manipal Academy of Higher Education, Manipal, Karnataka, India*

ABSTRACT: The growth of 5G communications has created a demand for advanced wearable and flexible antennas due to supporting the high speeds, low latency, and capability of mechanical deformation conditions such as bending and conformability. In this paper, the design and analysis of a defected ground structure (DGS)-based ring slot antenna for N77 (3.3–4.2 GHz) and N78 (3.3–3.8 GHz) frequency bands is demonstrated. The antenna is made of an RT/Duroid 5880 substrate and has a loss tangent ($\tan\delta$) of 0.0009 and dielectric constant (ε_r) of 2.2. A DGS-based ring slot microstrip antenna is simulated, tested, and experimentally characterized on different body locations (leg, chest, and hand) along with bending, and their results are presented accordingly. The magnitude of S_{11} ($|S_{11}|$) of the proposed antenna is -26.81 dB at resonant frequency of 3.45 GHz, with the impedance bandwidth of 22 MHz (3.486 GHz to 3.508 GHz), peak gain of 6.27 dBi, and radiation efficiency of 85.02%. The simulated specific absorption rate (SAR) for 1 g and 10 g human body tissues is 0.263 W/Kg and 0.076 W/Kg, respectively. The total volume of the antenna is $0.58\lambda_0 \times 0.58\lambda_0 \times 0.00595\lambda_0$ (at 3.5 GHz). The proposed antenna is suitable for 5G wearable devices.

1. INTRODUCTION

Wearable antennas are a groundbreaking advancement in antenna technology, designed to address the limitations of traditional rigid antennas [1, 2]. These antennas are lightweight, flexible, and can easily conform to different shapes and surfaces, making them ideal for the use in wearable devices and flexible electronics [3–5]. They often use materials like conductive fabrics, polymer composites, and stretchable substrates to achieve their flexibility. Key design considerations include maintaining performance despite bending or stretching, ensuring durability, and minimizing any interference with the wearer's comfort [6, 7]. As technology progresses, these antennas are becoming increasingly important for applications such as health monitoring, smart textiles, consumer electronics, fitness tracking, and 5G devices [8, 9].

In the context of 5G devices, flexible and wearable antenna design takes a significant step forward. These antennas are built to integrate smoothly into wearable technology, providing high performance while accommodating the body movements. By using flexible materials and advanced design techniques, they can maintain efficient signal transmission and reception, even when being bent or stretched. This flexibility is crucial for 5G devices, which demands high data speeds and reliable connectivity [10–16]. N77 (3.3–4.2 GHz) and N78 (3.3–3.8 GHz) frequency bands are essential parts of the 5G spectrum, each serving a unique role. The N77 band of 5G spectrum provides a good balance of coverage and capacity, making it suitable for high-speed internet and network efficiency. The N78 band is particularly effective in dense urban areas, delivering fast and reliable 5G services [17–19]. Together, these bands support higher data rates, reduced latency, and improved performance for a range of applications [20].

Some antennas such as antipodal Vivaldi and split-ring shaped antennas [21, 22], slot Vivaldi antenna [23], L-shaped microwave antenna [24], terminal loop antenna [25], planar dipole antenna [26], different radiating shapes such as rectangular, triangular, hexadecimal etc. microstrip and monopole antennas [27–30] have been reported and described for wearable applications. Some wearable antennas [21–30] suffer from a complex antenna structure, poor impedance matching, large antenna size, low gains, and high SAR values. Therefore, the design of wearable antenna having simple geometrical structure, good reflection coefficient, high gain without additional reflecting structures, conformability, flexibility, resilience in bending situations, and low SAR values as per standards is a vital research motivation in the present scenario to cover N77 and N78 frequency bands of 5G spectrum.

In this paper, a ring slot wearable antenna loaded with DGS for N77 and N78 frequency band applications is demonstrated. The antenna is composed of a ring slot antenna, a microstrip feed line, and a defected ground structure. Initially, the ring slot

* Corresponding author: Dinesh Yadav (dinesh.yadav@jaipur.manipal.edu).

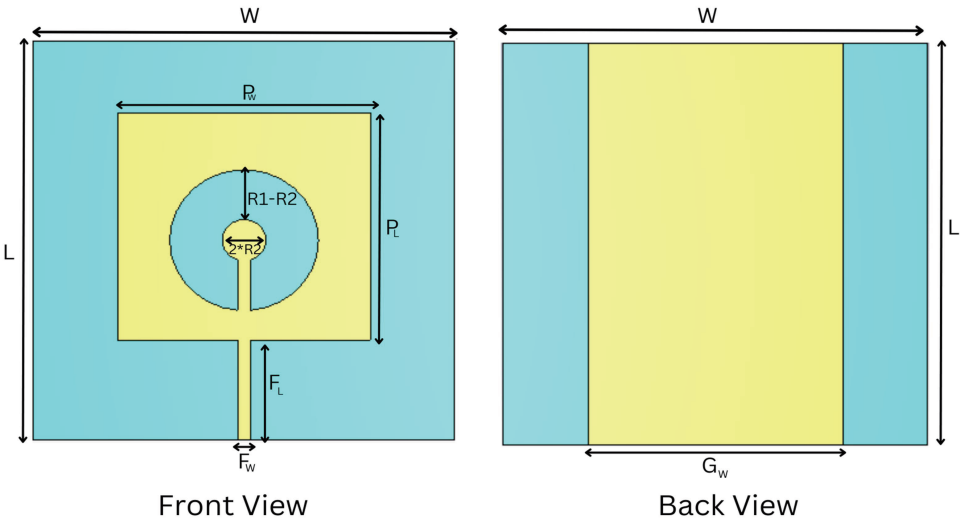

FIGURE 1. Layout of the proposed DGS-based ring slot microstrip antenna.

wearable antenna operates at 3.5 GHz and provides peak gain about 6.27 dBi. Subsequently, the antenna is tested under on-body conditions using a multilayer human body tissue model to analyze the SAR values of 1 g and 10 g tissues. Afterward, the on-body (when the antenna was in direct contact with the different parts of body) is made and bending analysis performed, and its impact on $|S_{11}|$ is presented. By focusing on advanced low-loss materials and design strategies, the study seeks to enhance the performance and reliability of 5G communication in wearable technology.

The rest of the paper is organized as follows. Section 2 covers the proposed ring slot antenna design and its analysis. In Section 3, the performance of the fabricated prototype is evaluated in off- and on-body environments and presented. Finally, Section 4 concludes the outcomes of the present study.

2. PROPOSED ANTENNA DESIGN AND ANALYSIS

The design layout (front and back views) of the proposed DGS-based ring slot wearable antenna is depicted in Figure 1. It is designed on a low-loss Roger RT/Duroid 5880 substrate having a relative permittivity (ε_r) of 2.2, a loss tangent ($\tan\delta$) of 0.0009, and a thickness of 0.508 mm. The radiating patch and ground plane are made of copper with a thickness of 0.035 mm, providing high conductivity and reliable performance. The fundamental antenna parameters, such as the resonant frequency and size of the proposed antenna, are initially calculated using the basic microstrip patch antenna design equations (Equations (1) to (6)). Following this, calculations for the ring slot are performed (Equations (7) to (12)). To achieve better impedance matching, further optimization is carried out after these initial calculations. The antenna is composed of a ring slot antenna, a microstrip feed line of width F_W for 50 Ω impedance matching on the front side and defected ground structure on the back side. CST Microwave Studio simulation software is utilized to perform the numerical analysis of the proposed antenna.

$$f_r = \frac{c}{2L\sqrt{\varepsilon_{eff}}} \tag{1}$$

$$W = \frac{c}{2f_r\sqrt{\frac{\varepsilon_r+1}{2}}} \tag{2}$$

$$\varepsilon_{eff} = \frac{\varepsilon_r+1}{2} + \frac{\varepsilon_r-1}{2}\left(1+12\frac{h}{W}\right)^{-1/2} \tag{3}$$

$$\Delta L = 0.412h\frac{(\varepsilon_{eff}+0.3)\left(\frac{W}{h}+0.264\right)}{(\varepsilon_{eff}-0.258)\left(\frac{W}{h}+0.8\right)} \tag{4}$$

$$L_{eff} = L + 2\Delta L \tag{5}$$

$$L = \frac{c}{2f_r\sqrt{\varepsilon_{eff}}} - 2\Delta L \tag{6}$$

where f_r is the resonant frequency, c the speed of light in a vacuum (3×10^8 m/s), ε_{eff} the effective dielectric constant of the substrate, h the height of the substrate, W width of the patch, ε_{eff} the effective dielectric constant, ε_r the relative permittivity (dielectric constant) of the substrate, ΔL the extension in patch length, L_{eff} the effective length of the patch, and L the length of the patch.

2.1. Equations Used for Design of a Ring Slot Antenna

$$\lambda_{eff} = \frac{c}{f_r\sqrt{\varepsilon_{eff}}} \tag{7}$$

$$r_{mean}\frac{r_i+r_o}{2} \tag{8}$$

For resonant frequency, the circumference of the mean ring should be approximately half the effective wavelength:

$$2\pi r_{mean} = \frac{\lambda_{eff}}{2}$$

TABLE 1. Optimized parameters of the proposed DGS-based ring slot microstrip antenna.

Parameter	L	W	P_L	P_W	F_L	F_W	$R1$	$R2$	G_W
Value (mm)	50	50	32	30	12.5	1.5	8.821	2.607	30

TABLE 2. Dielectric properties of four layer human tissues model at 3.45 GHz [5, 26].

Human Tissue	**Conductivity** σ **(S/m)**	**Dielectric constant** (ε_r)	**Mass Density** (Kg/m^3)	**Thickness (mm)**
Skin	1.44	37.88	1001	2
Fat	0.1	5.28	900	5
Muscle	1.74	52.73	1006	20
Bone	0.39	11.4	1008	13

$$r_{mean} = \frac{\lambda_{eff}}{4\pi} \quad (9)$$

$$r_o = r_{mean} + \frac{w_s}{2} \quad (10)$$

$$r_i = r_{mean} - \frac{w_s}{2} \quad (11)$$

$$w_s = r_o - r_i \quad (12)$$

where λ_{eff} is the effective wavelength, r_{mean} the mean radius of the ring, r_i the inner radius of the ring, r_o the outer radius of the ring, and w_s the slot width.

The total volume of the antenna is $50\,\text{mm} \times 50\,\text{mm} \times 0.508\,\text{mm}$, which is equivalent to $0.58\lambda_0 \times 0.58\lambda_0 \times 0.00595\lambda_0$, where λ_0 is the wavelength of the free space at 3.5 GHz. The optimized design parameters of the proposed DGS-based ring slot antenna are summarized in Table 1. The simulated reflection coefficient of the proposed antenna is illustrated in Figure 2. It can be seen that simulated $|S_{11}|$ of -20.99 dB at 3.5 GHz (resonating frequency, f_r) is perceived. From the study, it is perceived that the proposed antenna operates at 3.5 GHz which supports N77 and N78 frequency bands of 5G communication.

Figure 3 shows the simulated far-field gain pattern of the proposed antenna at 3.5 GHz. The far-field gain of 6.25 dBi in the $Phi = 0°$ plane (XZ-plane) with the far-field gain of 6.27 dBi in $Phi = 90°$ plane (YZ-plane) is perceived. It is also observed that far-field pattern in XZ-plane gives omnidirectional pattern with directional pattern in YZ-plane. These results indicate that the antenna provides consistent directional performance in YZ-plane and minimal variation in far-field gain in both planes.

Basically, SAR evaluates the electromagnetic energy absorbed by human tissues when they are exposed to the antenna radiation. In other words, SAR is a crucial parameter for assessing the safety of wearable devices, as it quantifies the rate at which electromagnetic energy is absorbed per unit mass of tissue, measured in watts per kilogram (W/Kg).

In order to analyze the SAR of the proposed ring slot antenna, the proposed ring slot antenna structure with multilayer human

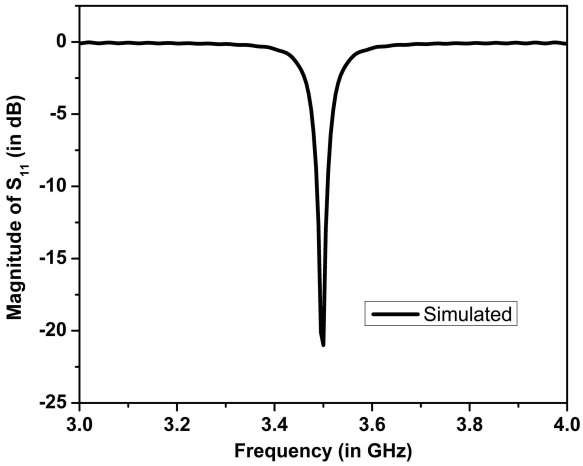

FIGURE 2. Simulated $|S_{11}|$ of the proposed DGS-based ring slot microstrip antenna.

tissue model is depicted in Figure 4(a). The multilayer structure of human tissue model contains four layers comprising skin, fat, muscle, and bone as shown in Figure 4 (b). The dielectric properties of four-layer human tissue model at 3.45 GHz are summarized in Table 2. This model is simulated on CST Microwave Studio Suite simulation software for the interaction between the proposed antenna and the human body tissue model. The utilized size of the human body tissue model is $50\,\text{mm} \times 50\,\text{mm}$ for the SAR calculation of 1 g and 10 g human tissues. The SAR analysis of 1 g and 10 g human tissues is presented in Figures 4(c) and (d), respectively. The simulated SAR values for the presented antenna are 0.263 W/Kg for 1 g tissues and 0.076 W/Kg for 10 g tissues. These values are well below the safety threshold of 1.6 W/Kg, as defined by international safety standards, including those set by the Federal Communications Commission (FCC). The low SAR values indicate that the antenna operates within safe limits, posing minimal risk of thermal effects on human tissues during prolonged exposure and makes the antenna highly suitable for wearable applications.

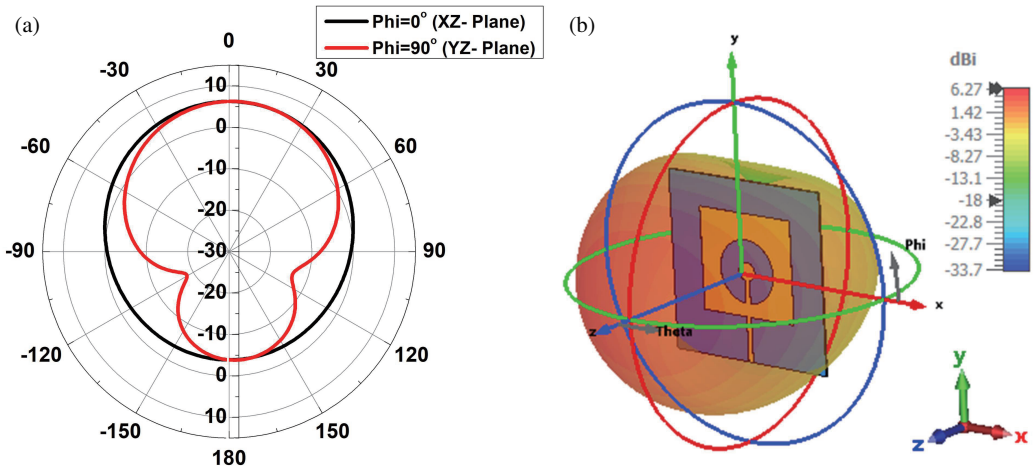

FIGURE 3. Simulated far-field gain pattern of the proposed ring slot antenna.

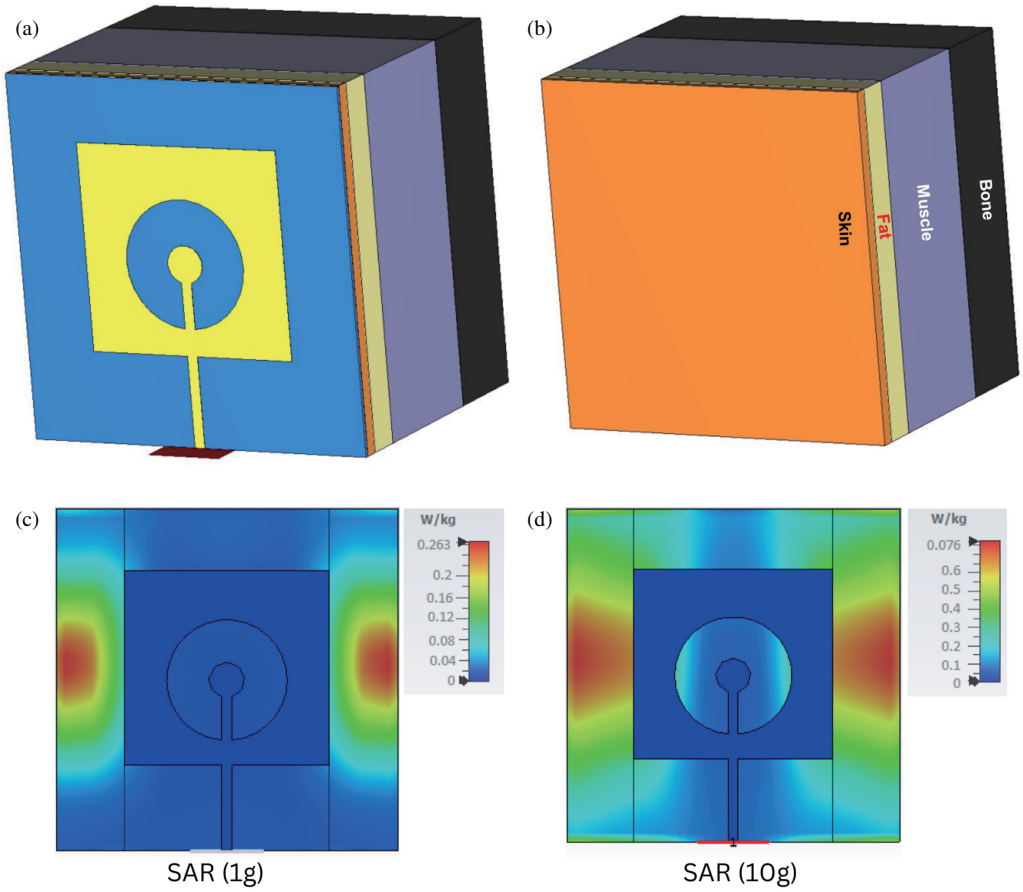

FIGURE 4. (a) Proposed ring slot antenna with multilayer human tissue model, (b) four layer human body tissues model, (c) SAR (1 g) analysis, and (d) SAR (10 g) analysis.

3. MEASURED RESULTS AND PERFORMANCE ANALYSIS

The proposed DGS-based ring slot antenna has been fabricated on an RT/duroid 5880 substrate using photolithography process. The front and back view photographs of the fabricated antenna are shown in Figures 5(a) and (b), respectively. Its $|S_{11}|$ performance is measured using calibrated N5234A PNA-L network analyzer, and the setup utilized for measurement is depicted in Figure 5(c). The simulated and measured $|S_{11}|$ of the proposed ring slot antenna are presented in Figure 5(d). The simulated $|S_{11}|$ is -20.99 dB at resonant frequency of 3.5 GHz whereas the measured $|S_{11}|$ is -26.81 dB at resonant frequency of 3.45 GHz. The mismatch between the simulated and mea-

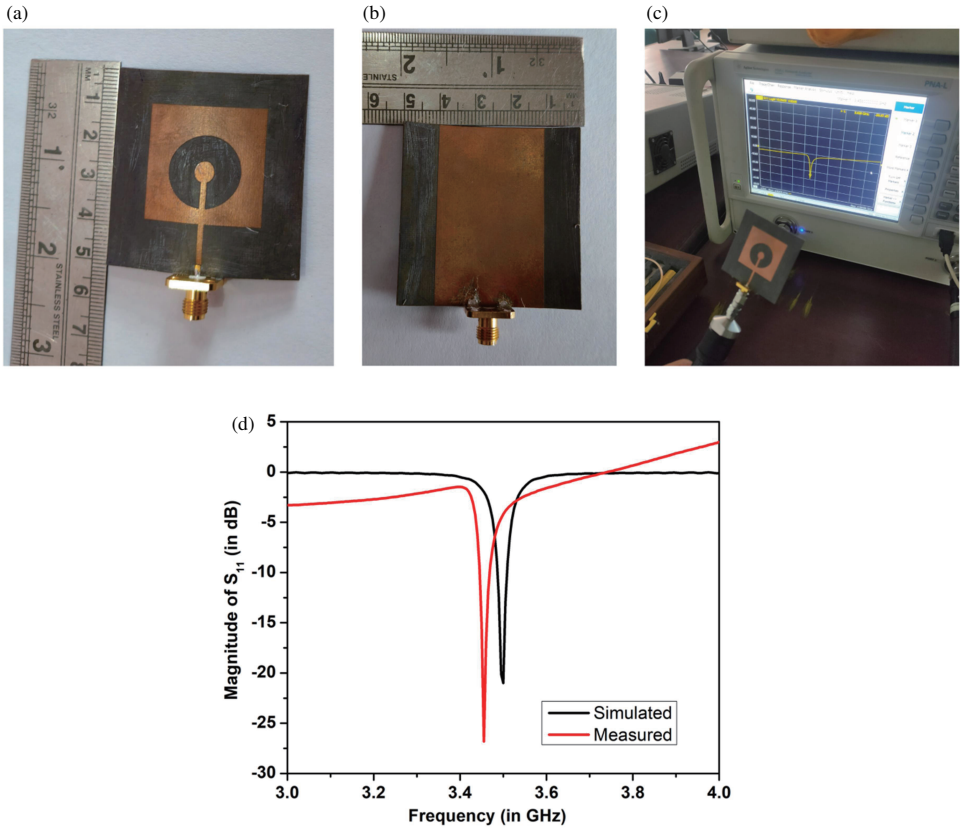

FIGURE 5. Fabricated antenna prototype, (a) front view, (b) back view, (c) measurement setup for $|S_{11}|$, and (d) simulated and measured $|S_{11}$.

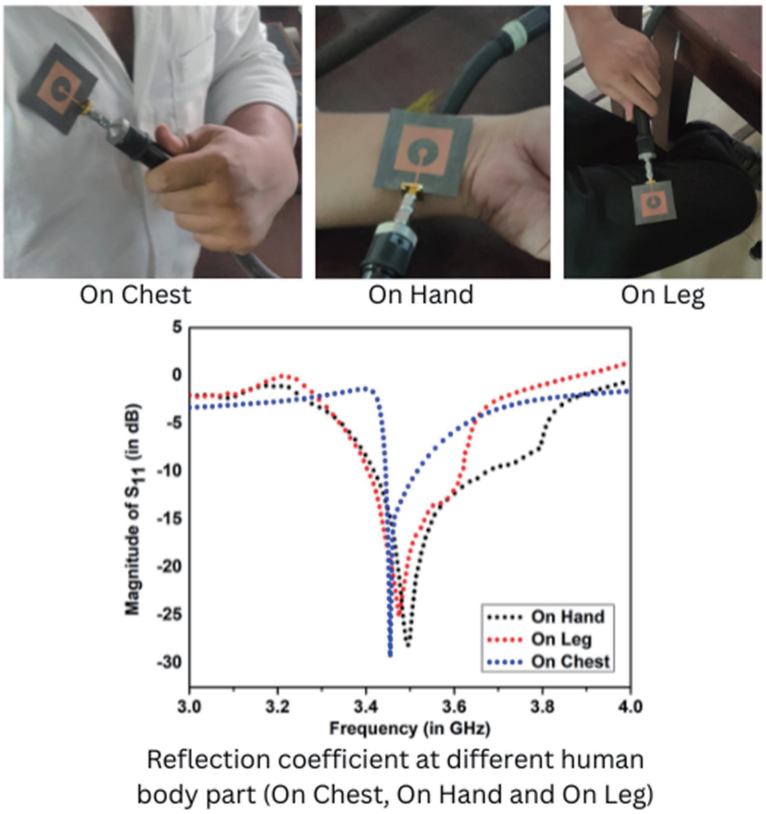

FIGURE 6. On-body performance analysis of the proposed ring slot antenna and their $|S_{11}$.

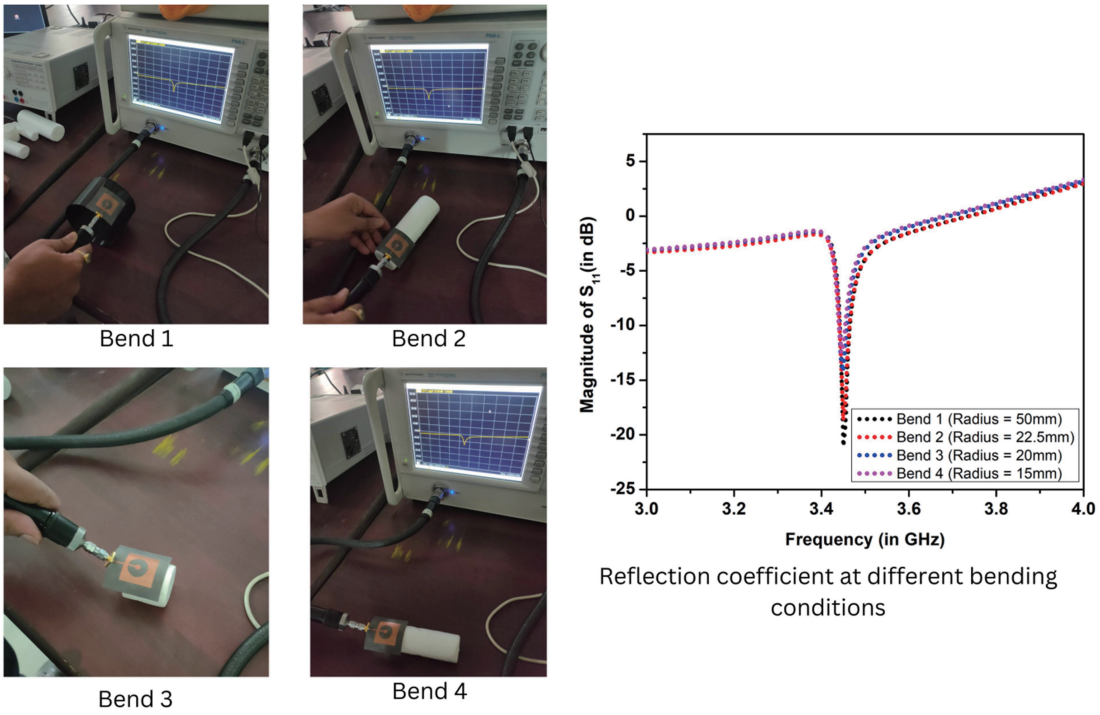

FIGURE 7. Different bending analysis of the proposed ring slot antenna and their $|S_{11}|$.

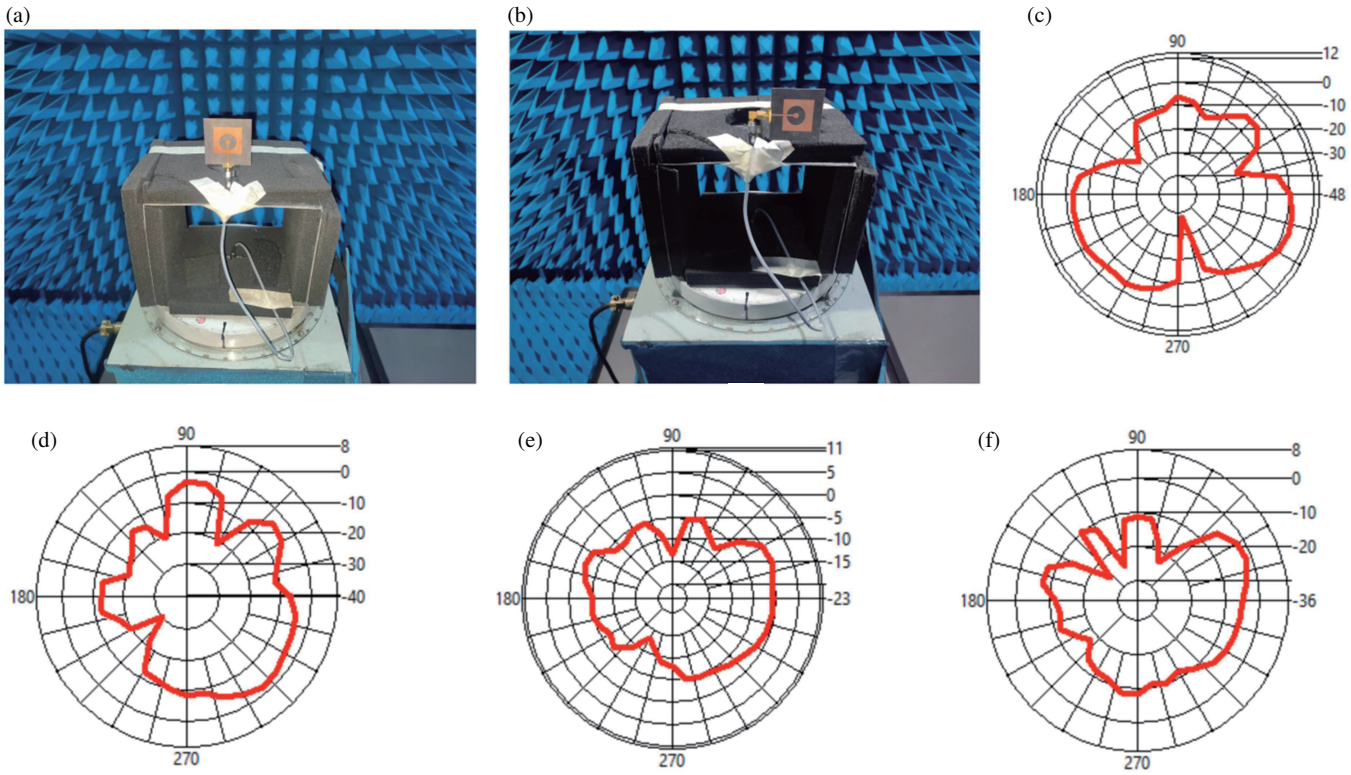

FIGURE 8. Measurement setup of the proposed antenna in anechoic chamber, (a) XZ-plane, (b) YZ-plane, (c) measured co-pol pattern in YZ-plane, (d) measured cross-pol pattern in YZ-plane, (e) measured co-pol pattern in XZ-plane, (f) measured cross-pol pattern in XZ-plane.

sured $|S_{11}|$ in Figure 5 is mainly due to fabrication tolerances, variations in the measurement environment, and imperfections in soldering or connectors.

The on-body performance analysis of the proposed ring slot antenna is conducted by placing the antenna at various positions such as chest, hand, and leg of human body in open environ-

TABLE 3. Comparative analysis of the proposed ring slot antenna with previous published works.

Ref. No.	Antenna footprint ($L \times W \times h$ mm^3)	Antenna Structure	Substrate Material	Operating frequency (GHz)	$\|S_{11}\|$ (dB)	Gain (dBi)	SAR (W/Kg) 1 g/10 g	On Body Performance Analysis
[21]	$0.385\lambda_0 \times 0.385\lambda_0 \times 0.00467\lambda_0$	Antipodal Vivaldi antenna	Polyester	3.5	-29.33	2.64	—	No
[22]	$0.817\lambda_0 \times 0.817\lambda_0 \times 0.035\lambda_0$	Split ring-shaped antenna	Felt	3.5	-42	6	—	No
[23]	$0.525\lambda_0 \times 0.525\lambda_0 \times 0.00467\lambda_0$	Slot Vivaldi antenna	Polyester	3.5	-20	4.7	—	No
[24]	$0.525\lambda_0 \times 0.525\lambda_0 \times 0.00467\lambda_0$	Slot Vivaldi antenna	Polylactic acid (PLA)	3.5	-23.69	5.68	—	No
[25]	$0.735\lambda_0 \times 0.653\lambda_0 \times 0.00583\lambda_0$	L-shaped Microwave antenna	Polycarbonate	3.5	-15	3.1	—	No
[26]	$1.633\lambda_0 \times 0.840\lambda_0 \times 0.0183\lambda_0$	Terminal Loop antenna	FR4	4.9	-20	—	0.358/ 0.293	Yes
[27]	$0.677\lambda_0 \times 0.467\lambda_0 \times 0.041\lambda_0$	Planar dipole antenna	Nitrile butadiene rubber (NBR) polymer	2.44	-17.77	1.38	0.864/0.273	Yes
[28]	$0.817\lambda_0 \times 0.817\lambda_0 \times 0.0233\lambda_0$	Microstrip patch antenna	Wool Felt	3.5	-20	1.38	0.533/-	Yes
[29]	$0.42\lambda_0 \times 0.21\lambda_0 \times 0.00233\lambda_0$	Triangular monopole antenna	Rogers ULTRALAM 3850	3.5	-14.62	2.262	0.903/-	Yes
[30]	$0.467\lambda_0 \times 0.35\lambda_0 \times 0.00315\lambda_0$	Hexagonal shaped microstrip antenna	Photopaper	3.5	-19	2.24	1.98/1.53	Yes
Our work	$0.58\lambda_0 \times 0.58\lambda_0 \times 0.00595\lambda_0$	DGS-based ring slot antenna	RT/Duroid 5880	3.5	-26.81	6.27	0.263/0.076	Yes

ment. Figure 6 illustrates the measurement setup for these on-body tests, including the antenna placements on the hand, leg, and chest, along with their corresponding $|S_{11}|$ measurements. The measured $|S_{11}|$ is -29.38 dB at 3.46 GHz when the antenna is placed on the chest. Correspondingly, the measured $|S_{11}|$ are -28.17 dB at 3.49 GHz and -25.16 dB at 3.47 GHz on the hand and leg, respectively. It can be perceived that the antenna has consistent performance in terms of resonant frequency while the reflection coefficient is slightly deteriorated by placing the antenna on the hand and leg positions. The study demonstrates that the antenna has consistent performance across different body locations, confirming its suitability for wearable applications.

Bending affects the effective permittivity and surface current distribution, leading to shifts in resonance frequency and impedance matching. Increased bending introduces mechanical strain, causing minor performance degradation. These theoretical insights align with our experimental results, which show slight variations in $|S_{11}|$ and resonant frequency, but overall, the antenna maintains its suitability for flexible and wearable applications.

To assess the conformability of the proposed ring slot antenna, a series of bending tests were conducted using foam cylinders of varying diameters. The antenna was bent around different cylindrical forms to evaluate its performance under mechanical stress. Specifically, the antenna was bent around a 100 mm diameter PVC plastic cylinder for Bend 1, a 45 mm diameter cylindrical foam pipe for Bend 2, a 40 mm diameter cylindrical foam pipe for Bend 3, and a 30 mm diameter cylindrical foam pipe for Bend 4. The details of this bending analysis and their $|S_{11}|$ are illustrated in Figure 7. At resonant frequency of 3.45 GHz, the measured $|S_{11}|$ were -21.04 dB for Bend 1, -18.69 dB for Bend 2, -14.19 dB for Bend 3, and -11.98 dB for Bend 4. These results demonstrate how the antenna performance varies with different levels of bending, highlighting its flexibility.

Figures 8(a) and (b) illustrates the measurement setup used in anechoic chamber to evaluate the radiation patterns in XZ-plane ($Phi = 0°$) and YZ-plane ($Phi = 90°$) of the proposed ring slot antenna, respectively. Figures 8(c) to (d) presents the co-polarized (co-pol) and cross-polarized (cross-pol) radiation pattern in the YZ-plane, respectively. Whereas the co-polarized (co-pol) and cross-polarized (cross-pol) radiation pattern in the XZ-plane are shown in Figures 8(e) to (f), respectively. In YZ-plane, the directional radiation pattern at 3.45 GHz is depicted in Figure 9. It can be perceived that directional radiation patterns in YZ-plane and omnidirectional in XZ-plane.

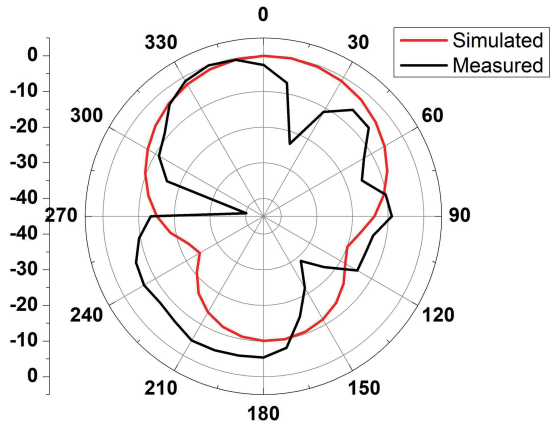

FIGURE 9. Radiation pattern at 3.45 GHz of the proposed ring slot antenna.

In Table 3, the performance of the proposed DGS-based ring slot wearable antenna is compared with the previously published wearable antennas. In [26], it is difficult for the antenna to confirm to the human body as the substrate is rigid. In [21–30], compared with the proposed ring slot wearable antenna, the cited antennas suffer from a complex structure, slightly large size, low gains, and high SAR values. Therefore, the proposed ring slot antenna has advantages of simple structure, good impedance matching of -26.81 dB, high peak gain of 6.27 dBi, and low SAR values of 0.263 W/Kg (1 g) and 0.076 W/Kg (10 g) tissues. With these excellent features, the proposed ring slot antenna may meet the demands of N77 and N78 5G wearable applications.

4. CONCLUSION

In this paper, a DGS-based ring slot antenna is designed and experimentally tested for 5G communication in the N77 and N78 frequency bands. The measured $|S_{11}|$ is -26.81 dB at 3.45 GHz, peak gain of 6.27 dBi, and radiation efficiency of 85.02% while maintain the electrical size of $0.58\lambda_0 \times 0.58\lambda_0 \times 0.00595\lambda_0$. The SAR of the proposed antenna is presented and perceived the 0.263 W/Kg for 1 g body tissue and 0.076 W/Kg for 10 g body tissue. The bending and on-body performance of the proposed antenna is optimized and presented. It is perceived that the stable performance in $|S_{11}|$ while placing the proposed antenna at various positions on human body in open environment. Based on the study, the proposed antenna is potentially suitable for wearable 5G applications.

REFERENCES

[1] Giftsy, A. L. S., U. K. Kommuri, and R. P. Dwivedi, "Flexible and wearable antenna for biomedical application: Progress and opportunity," *IEEE Access*, Vol. 12, 90 016–90 040, 2023.

[2] Lee, H. and Y. B. Park, "Wideband ring-monopole flexible antenna with stub for WLAN/C-Band/X-Band applications," *Applied Sciences*, Vol. 12, No. 21, 10717, 2022.

[3] Tiwari, R. N., D. Sharma, P. Singh, and P. Kumar, "Design of dual-band 4-port flexible MIMO antenna for mm-Wave technologies and wearable electronics," *IEEE Access*, Vol. 12, 96 649–96 659, 2024.

[4] Paracha, K. N., S. K. A. Rahim, P. J. Soh, and M. Khalily, "Wearable antennas: A review of materials, structures, and innovative features for autonomous communication and sensing," *IEEE Access*, Vol. 7, 56 694–56 712, 2019.

[5] Soni, G. K., D. Yadav, and A. Kumar, "Design consideration and recent developments in flexible, transparent and wearable antenna technology: A review," *Transactions on Emerging Telecommunications Technologies*, Vol. 35, No. 1, e4894, 2024.

[6] Yu, Z., R. Niu, G. Zhang, R. Sun, Z. Lin, Y. Li, and X. Ran, "A wearable self-grounding slit antenna for ISM/4G/5G/bluetooth/WLAN applications," *IEEE Access*, Vol. 11, 87 930–87 937, 2023.

[7] Tiwari, R. N., P. Singh, B. K. Kanaujia, and A. K. Pandit, "A coalesced kite shaped monopole antenna for UWB technology," *Wireless Personal Communications*, Vol. 114, No. 4, 3031–3048, 2020.

[8] Sharma, D., R. N. Tiwari, S. Kumar, S. Sharma, and L. Matekovits, "A compact wearable textile antenna for NB-IoT and ISM band patient tracking applications," *Sensors*, Vol. 24, No. 15, 5077, 2024.

[9] Ali, U., S. Ullah, B. Kamal, L. Matekovits, and A. Altaf, "Design, analysis and applications of wearable antennas: A review," *IEEE Access*, Vol. 11, 14 458–14 486, 2023.

[10] Qiu, H., H. Liu, X. Jia, Z.-Y. Jiang, Y.-H. Liu, J. Xu, T. Lu, M. Shao, T.-L. Ren, and K. J. Chen, "Compact, flexible, and transparent antennas based on embedded metallic mesh for wearable devices in 5G wireless network," *IEEE Transactions on Antennas and Propagation*, Vol. 69, No. 4, 1864–1873, Apr. 2021.

[11] Sun, H., Z. Zhang, R. Q. Hu, and Y. Qian, "Wearable communications in 5G: Challenges and enabling technologies," *Ieee Vehicular Technology Magazine*, Vol. 13, No. 3, 100–109, Sep. 2018.

[12] Yu, Z., R. Niu, G. Zhang, R. Sun, Z. Lin, Y. Li, and X. Ran, "A wearable self-grounding slit antenna for ISM/4G/5G/bluetooth/WLAN applications," *IEEE Access*, Vol. 11, 87 930–87 937, 2023.

[13] Sharma, P., R. N. Tiwari, P. Singh, and P. Kumar, "Trident-shaped dual band monopole antenna with defected ground plane for 5G applications," in *2022 IEEE Wireless Antenna and Microwave Symposium (WAMS)*, 1–4, Rourkela, India, 2022.

[14] Muduli, A., M. K. Kanneboina, K. V. Mudumunthala, and S. Valluri, "A reconfigurable wearable antenna for mid band 5G applications," in *Journal of Physics: Conference Series*, Vol. 1921, No. 1, 012051, 2021.

[15] Hughes, J. D., C. Occhiuzzi, J. Batchelor, and G. Marrocco, "Twin-grid array as 3.6 GHz epidermal antenna for potential backscattering 5G communication," *IEEE Antennas and Wireless Propagation Letters*, Vol. 19, No. 12, 2092–2096, Dec. 2020.

[16] Mallat, N. K., A. Jafarieh, H. Noorollahi, and M. Nouri, "A novel fractal arrow-shaped mmWave flexible antenna for IoT and 5G communication systems," *Progress In Electromagnetics Re-*

search Letters, Vol. 107, 9–17, 2022.

[17] Zade, P. L. and S. S. Khade, "Miniaturized novel multi resonance monopole planar antenna with slots, slits, split ring resonator," *Progress In Electromagnetics Research C*, Vol. 145, 75–82, 2024.

[18] Gollamudi, N. K., Y. V. Narayana, and A. M. Prasad, "A novel cow-head shaped multiple input multiple output antenna for 5G Sub: 6 GHz N77/N78 & N79 bands applications," *Progress In Electromagnetics Research C*, Vol. 122, 83–93, 2022.

[19] Sim, C.-Y.-D., H.-Y. Liu, and C.-J. Huang, "Wideband MIMO antenna array design for future mobile devices operating in the 5G NR frequency bands n77/n78/n79 and LTE band 46," *IEEE Antennas and Wireless Propagation Letters*, Vol. 19, No. 1, 74–78, 2019.

[20] Sun, J.-N., J.-L. Li, and L. Xia, "A dual-polarized magneto-electric dipole antenna for application to N77/N78 band," *IEEE Access*, Vol. 7, 161 708–161 715, 2019.

[21] Sahoo, B. C., A. A. Al-Hadi, S. N. Azemi, W. F. Hoon, S. Padmanathan, C. M. N. C. Isa, S. Afroz, Y. S. Loh, M. I. Suhaimi, L. M. Lim, Z. Samsudin, I. Mansor, and P. J. Soh, "Compact wideband wearable antipodal Vivaldi antenna for 5G applications," in *2022 IEEE International RF and Microwave Conference (RFM)*, 1–4, Kuala Lumpur, Malaysia, 2022.

[22] Mashaghba, H. A., H. A. Rahim, P. J. Soh, M. Abdulmalek, I. Adam, M. Jusoh, T. Sabapathy, M. N. M. Yasin, and K. N. A. Rani, "Bending assessment of dual-band split ring-shaped and bar slotted all-textile antenna for off-body WBAN/WLAN and 5G applications," in *2020 2nd International Conference on Broadband Communications, Wireless Sensors and Powering (BCWSP)*, 1–5, Yogyakarta, Indonesia, 2020.

[23] Sahoo, B. C., A. A. Al-Hadi, S. N. Azemi, W. F. Hoon, S. Padmanathan, C. M. N. C. Isa, S. Afroz, Y. S. Loh, M. S. Mahyuddin, L. M. Lim, Z. Samsudin, I. Mansor, and P. J. Soh, "Compact full flexible Vivaldi antenna for 3.5 GHz wearable applications," in *2023 IEEE International Symposium On Antennas And Propagation (ISAP)*, 1–2, Kuala Lumpur, Malaysia, 2023.

[24] Othman, M. A., N. A. S. Ruslan, M. H. Misran, M. A. M. Said, R. A. Manap, A. S. Jaafar, N. I. Hassan, and S. Suhaimi, "3.5 GHz Vivaldi antennas: A comprehensive parametric analysis for unleashing 5G communication technology," *ASEAN Engineering Journal*, Vol. 13, No. 3, 159–163, 2023.

[25] Malik, S. A., K. Muzaffar, A. H. Mir, and A. H. Moon, "Extremely close integration of dual band sub-6 GHz 4G antenna with unidirectional mmWave 5G antenna," *Progress In Electromagnetics Research Letters*, Vol. 96, 73–80, 2021.

[26] Pang, B., W. Hu, W. Jiang, and B. Lu, "Design of low-SAR terminal antenna using characteristic mode manipulation," *IEEE Antennas and Wireless Propagation Letters*, Vol. 22, No. 4, 749–753, Apr. 2023.

[27] Al-Sehemi, A. G., A. A. Al-Ghamdi, N. T. Dishovsky, N. T. Atanasov, and G. L. Atanasova, "Flexible and small wearable antenna for wireless body area network applications," *Journal of Electromagnetic Waves and Applications*, Vol. 31, No. 11-12, 1063–1082, 2017.

[28] Yang, H. and X. Liu, "Wearable dual-band and dual-polarized textile antenna for on-and off-body communications," *IEEE Antennas and Wireless Propagation Letters*, Vol. 19, No. 12, 2324–2328, Dec. 2020.

[29] El Atrash, M., M. A. Abdalla, and H. M. Elhennawy, "A wearable dual-band low profile high gain low SAR antenna AMC-backed for WBAN applications," *IEEE Transactions on Antennas and Propagation*, Vol. 67, No. 10, 6378–6388, Oct. 2019.

[30] Jabbar, A., M. Zubair, M. A. Naveed, M. Q. Mehmood, and Y. Massoud, "A photopaper-based low-cost, wideband wearable antenna for wireless body area network applications," *IET Microwaves, Antennas & Propagation*, Vol. 16, No. 15, 962–970, 2022.